END
DATE
FILMED
12-81
DTIC

LEVEL

AD A106679

PARAMETRIC CONSIDERATIONS FOR INDUCTIVELY DRIVEN PLASMA IMPLOSIONS

R. E. Reinovsky
D. L. Smith

January 1981

Final Report

DTIC
SELECTED
NOV 4 1981

A

Approved for public release; distribution unlimited.

DTIC FILE COPY

AIR FORCE WEAPONS LABORATORY
Air Force Systems Command
Kirtland Air Force Base, NM 87117

81 11 02 076

This final report was prepared by the Air Force Weapons Laboratory, Kirtland Air Force Base, New Mexico, under Job Order 12091101. Dr. Robert E. Reinovsky (NTYP) was the Laboratory Project Officer-in-Charge.

This technical report has been reviewed and is approved for publication.

ROBERT E. REINOVSKY, PhD
Project Officer

N. F. RODERICK
Lt Colonel, USAF
Chief, Advanced Concepts Branch

FOR THE DIRECTOR

N. K. BLOCKER
Colonel, USAF
Chief, Applied Physics Division

REPORT DOCUMENTATION PAGE		READ INSTRUCTIONS BEFORE COMPLETING FORM
1. REPORT NUMBER AFWL-TR-79-179	2. GOVT ACCESSION NO. AD-A106679	3. RECIPIENT'S CATALOG NUMBER
4. TITLE (and Subtitle) PARAMETRIC CONSIDERATIONS FOR INDUCTIVELY DRIVEN PLASMA IMPLOSIONS.		5. TYPE OF REPORT & PERIOD COVERED Final Report.
		6. PERFORMING ORG. REPORT NUMBER
7. AUTHOR(s) R. E. Reinovsky D. L. Smith		8. CONTRACT OR GRANT NUMBER(s)
9. PERFORMING ORGANIZATION NAME AND ADDRESS Air Force Weapons Laboratory (NTYP) Kirtland Air Force Base, NM 87117		10. PROGRAM ELEMENT, PROJECT, TASK AREA & WORK UNIT NUMBERS 64746F/1209/101
11. CONTROLLING OFFICE NAME AND ADDRESS Air Force Weapons Laboratory (NTYP) Kirtland Air Force Base, NM 87117		12. REPORT DATE January 1981
		13. NUMBER OF PAGES 36
14. MONITORING AGENCY NAME & ADDRESS(if different from Controlling Office)		15. SECURITY CLASS. (of this report) Unclassified
		15a. DECLASSIFICATION/DOWNGRADING SCHEDULE

16. DISTRIBUTION STATEMENT (of this Report)

Approved for public release; distribution unlimited.

17. DISTRIBUTION STATEMENT (of the abstract entered in Block 20, if different from Report)

18. SUPPLEMENTARY NOTES

19. KEY WORDS (Continue on reverse side if necessary and identify by block number)

Opening Switches
Pulsed Power
Inductive Storage

20. ABSTRACT (Continue on reverse side if necessary and identify by block number)

This report explores the system aspects of driving implosion loads with
inductive sources. High-speed plasma implosions represent an attractive
approach to the production of an intense radiation source for use in an X-ray
Effects Simulator. The nature of the implosion and the energy levels
required for an X-ray Simulator make the use of inductive energy sources for
driving the implosion attractive from the standpoints of both physics and
economics. Parametric analysis and circuit calculations are employed to (over)

DD FORM 1473

20. ABSTRACT (Continued)

investigate the interrelation of circuit parameters (storage and load inductances), load parameters (mass, size, and speed), and switch parameters (resistance and rise time). The results show that 25 percent inductive to kinetic efficiency is attainable with only moderate requirements placed upon the switch performance. The status of current opening switch development is reviewed, and meets the minimum requirements predicted by the analysis.

CONTENTS

ILLUSTRATIONS

I. INTRODUCTION

Future applications of SHIVA-type electromagnetically driven plasma implosion, including the design of a full-scale nuclear environmental simulator, will require the storage and delivery of exceedingly large amounts of electrical energy. As presently envisioned, the minimum useful radiation output of 5-10 MJ from such a simulator implies delivered electrical energies of 15-30 MJ. Using design philosophies explored in previous work (Ref. 1), this level of delivered electrical energy implies that energies of 30-60 MJ must be stored in a form from which they can be delivered in microsecond time scales. Based on recent estimates, this probably results in a system costing $100 million and occupying a volume of 54,000 m^3 (70 m dia x 14 m high).

An attractive alternative technology for supplying large amounts of energy may be conceptually developed using inductive (magnetic) energy conditioning techniques coupled with inertial primary energy storage. The inertial primary store is essentially present technology. Therefore, the purpose of this report is to explore the potential applicability of inductive pulse-forming techniques for driving imploding plasma loads. Special attention is paid to the critical problem area in the system, which is the development of a suitable opening switch to deliver power to the load.

The inductive store driving a cylindrical implosion system is particularly amenable to analytic modeling, and the first section of this report discusses the implication of such models. The results, while encouraging in themselves, imply rather severe operational requirements for the opening switch. These requirements appear well beyond currently existing technology. The second section of this report deals with the investigation of more detailed models which require numerical solutions. The more detailed models address more quantitatively the influence of switch behavior on load performance. Considerably more latitude is allowed than is suggested by simple analytical models. The last section discusses existing data on the performance of opening switches in light of the performance required by the models.

---

1. Reinovsky, R. E., Conceptual Design of a 6 MJ Pulse Power System for Driving SHIVA, AFWL-DYP-TN-78-126, Air Force Weapons Laboratory, Kirtland Air Force Base, New Mex, December 1978.

II. ANALYSIS

This section explores the concept of inductively driven imploding loads using the simplest analytic circuit models. This analysis differs slightly from the familiar analysis of the inductive-store/inductive-load problem in that it allows for a load whose inductance increases subsequent to the initiation of current interruption in the primary circuit. The practical circuit under consideration is shown in Figure 1. It consists of a d.c. charged capacitor bank (C) discharged through an inductor (L_s) and a switch which is initially closed but will open to transfer energy. The inductor includes the internal inductance of the bank (L_1) and may be augmented by additional storage inductance (L_{ext}). Thus, the energy stored in the parasitic bank inductance is made available to the circuit. An initially open output switch S_2 isolates the load from the charging system prior to switching time t_s. The load inductance $L_{(t)}$ consists of a nonzero initial inductance L_o and a time varying inductance $\Delta L_{(t)}$ corresponding to the implosion of the foil/plasma. The ΔL in nH is given by

$$\Delta L_{(t_p)} = 2 \ h \ \ln\left(\frac{R_o}{R_f}\right)$$

where R_f is the final radius of the pinch, R_o is the initial radius of the foil cylinder, and h is the height of the foil cylinder in cm. The ratio R_o/R_f, referred to as the convergence ratio, is controlled by magnetohydrodynamics (MHD) considerations and typically lies between 10 and 20. For implosion times, greater than 1 μs a convergence of 7-12 is common; and, for shorter time scales, improved stability is expected to lead to slightly higher convergences.

In operation, energy is transferred from C to L_s and S_1 is opened at peak current (I_o). At peak current the voltage on C is near zero; and, if the energy transfer to the load is fast compared to the L_sC time constant, then the amount by which the charge on C can charge (i.e., $\Delta Q = I_o\Delta t$) is small and the voltage on C can be assumed to be near zero and to remain near zero during all time of interest. Thus, the practical circuit in Figure 1 is reduced to the equivalent circuit in Figure 2.

4
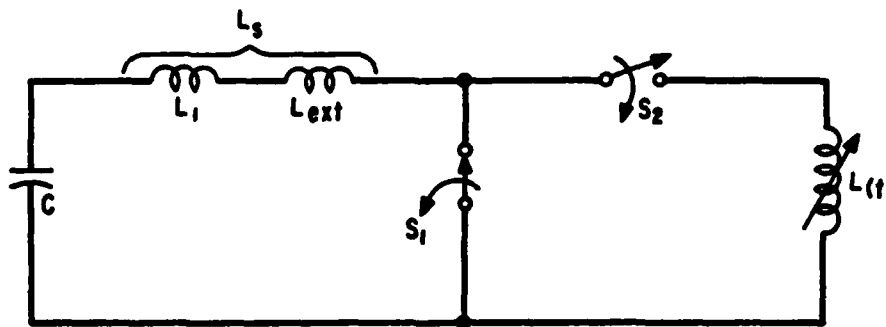
Figure 1. General inductive energy storage circuit.
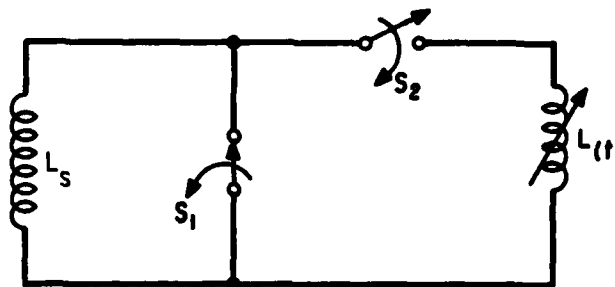
Figure 2. Equivalent circuit.

Approach the analysis of the circuit in Figure 2 in a two-step process. In each step, conservation of magnetic flux is assumed. The first step is the opening of the switch S_1 which is considered a resistor whose resistance goes from zero to infinity rapidly. The second step is the implosion, with S_1 effectively out of the circuit and S_2 closed, in which $L_{(t)}$ goes from L_0 to $(L_0 + \Delta L)$. Prior to the opening of S_1 the energy stored in L_s is

$$E_0 = \frac{L_s}{2} I_0{}^2 \tag{1}$$

After S_1 opens and S_2 closes at t_s, the current flowing assumes a new value I_1 given by

$$I_1 = \frac{L_s}{L_s + L_0} I_0 \tag{2}$$

I_1 is flowing in both L_s and $L_{(t)}$ where $L(t_s) = L_0$. Thus the energy stored in inductors L_s and L_0 is

$$E_1 = \frac{L_s}{L_s + L_0} \, E_0 \tag{3}$$

and the energy dissipated in the switch resistance as it climbs to infinity is

$$E_{switch} = \frac{L_0}{L_s + L_0} \, E_0 \tag{4}$$

Note that to minimize the energy lost in the interruption and transfer L_0 should be as low as possible.

After the implosion, the value of $L_{(t)}$ has risen to $L_0 + \Delta L$, the current has dropped to I_2,

$$I_2 = \frac{L_s}{L_s + L_0 + \Delta L} \, I_0 \tag{5}$$

and the energy remaining in the magnetic field of L_s, L_0 and ΔL is only

$$E_2 = \frac{L_s}{L_s + L_0 + \Delta L} \, E_0 \tag{6}$$

The difference in energy $E_1 - E_2$ is the energy dissipated in doing work on the load inductance $L_{(t)}$ to increase its value from L_0 to $(L_0 + \Delta L)$. Thus, $E_1 - E_2$ is just the kinetic energy coupled to the plasma shell during the implosion.

$$E_{ke} = \left(\frac{L_s}{L_s + L_0} - \frac{L_s}{L_s + L_0 + \Delta L} \right) E_0 \tag{7}$$

A kinetic efficiency can be defined as the ratio of kinetic energy to inductively stored energy. Thus

$$n_{ke} = \frac{E_{ke}}{E_0} = \frac{L_s}{L_s + L_0} - \frac{L_s}{L_s + L_0 + \Delta L} \tag{8a}$$

$$n_{ke} = \frac{L_s \Delta L}{(L_s + L_0)(L_s + L_0 + \Delta L)} \tag{8b}$$

Recalling that $L_0 \ll L_s$ is desired, L_0 compared to L_s can be neglected, and

$$\eta_{ke} \approx \frac{\Delta L}{L_s + \Delta L} \qquad (9)$$

Thus, if ΔL can be made much larger than L_s ($L_s \ll \Delta L$), then $\eta_{ke} \to 1$, and we can in principle get virtually all the magnetically stored energy into kinetic energy. Thus, in general, high efficiency requires

$$L_0 \ll L_s \ll \Delta L \qquad (10)$$

L_0 is in general fixed by the mechanical and electrical consideration of power flow to the load, while ΔL is fixed by the convergence ratio and the length. Usually values of L_0 below 3-5 nH are unrealistic, while conversion ratios of 20 and a length of a few (1-4) cm results in ΔL of 6-24 nH. Thus, in practice, the criteria cannot be easily satisfied to produce very high efficiency.

The value of L_s remains as one parameter which can be adjusted. If L_s is chosen to be very small, a large amount of energy is lost in the switching operation; if it is chosen to be large, the energy transfer to the load suffers. To find the optimum choice of L_s we take $d\eta_{ke}/dL_s$ and set the result equal to zero. This results in a criterion for L_s, namely:

$$L_s = \sqrt{L_0^2 + L_0 \, \Delta L} \qquad (11)$$

For the case of the static load, $\Delta L = 0$, Equation 11 gives $L_s = L_0$. Thus the familiar static result is recovered; and, as expected from Equations 2-4,

$$E_1 = 50\% \; E_0 \qquad (12a)$$

$$E_{switch} = 50\% \; E_0 \qquad (12b)$$

Figure 3 is a plot of η_{ke} as a function of L_s for an implosion where $\Delta L = 12$ nH and for values of L_0 of 1, 3, and 5 nH. The figure shows that the efficiency of coupling inductive to kinetic energy goes through a maximum at the predicted optimum L_s and that the optimum is quite broad, generally losing less than 10 percent of peak efficiency for a factor of 2 deviation from optimum storage inductance. Thus, while designing to the optimum inductance is useful, precise matching is usually unnecessary.
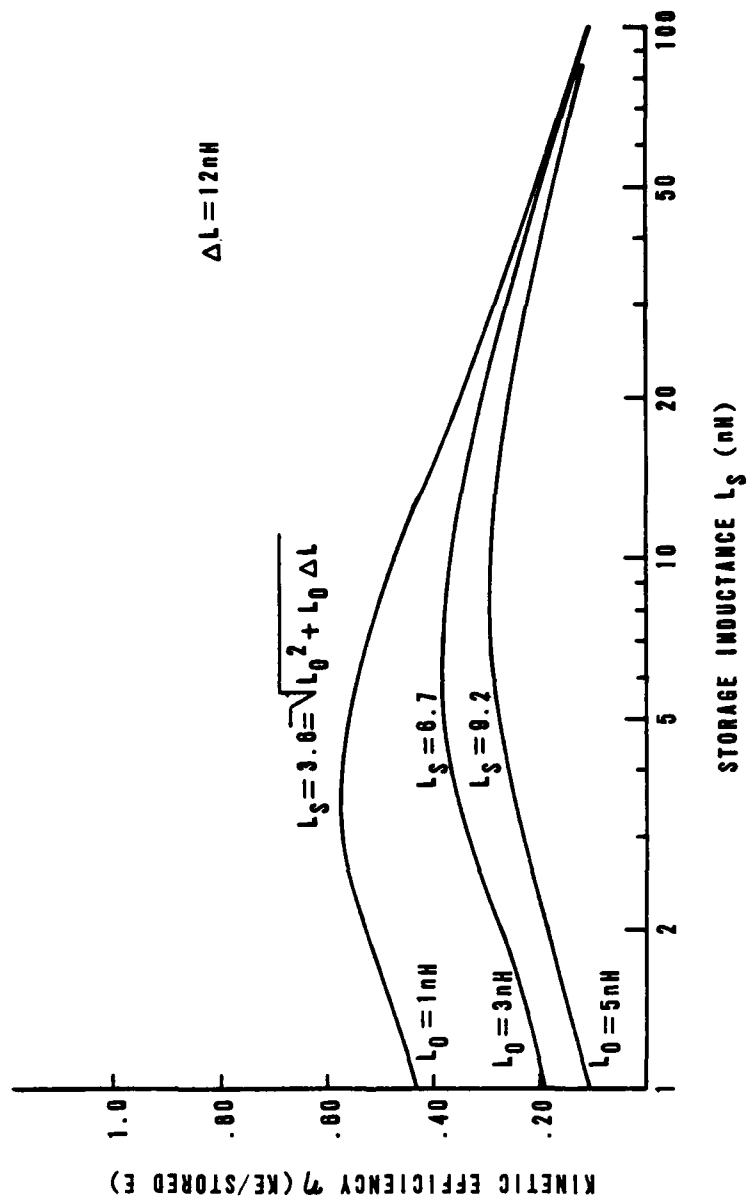
Figure 3. Kinetic efficiency vs storage inductance.

8

Equations 2-4 show that achieving values of L_o smaller than L_s is desirable, but that significantly reducing L_o is one of the harder tasks in system designs. The gain in efficiency to be achieved from lowering L_o must be evaluated quantitatively. Figure 4 is a plot of kinetic efficiency from Equation 8 (kinetic energy per unit inductively stored energy) versus ΔL for a range of L_o from 1-10 nH. As expected, η_{ke} increases with increasing ΔL and decreasing L_o. For ΔL of 12 nH (2 cm high, convergence of 20) the values of $L_o = 1$ give a very respectable efficiency of about 57 percent, while for $L_o = 10$ nH, the efficiency drops to less than 20 percent. This indicates that a decrease in L_o is an effective method of increasing efficiency.

The other method of increasing η_{ke} is by increasing ΔL. Since the conversion ratio is essentially fixed, ΔL can be increased by increasing the height, generally at little or no cost in increasing L_o. For example, doubling the height of a 2-cm load to 4 cm doubles ΔL from 12-24 nH, which for $L_o = 5$ nH increases η_{ke} from 30 to 42 percent. For those applications where kinetic energy per unit length is a criterion in addition to total kinetic energy, the process of lengthening the foil actually results in a decrease in kinetic energy per unit length, and is therefore not a useful approach.

For electrically exploded conductors, the operation of the switch is determined by the energy (and to some extent power history) dissipated in the switch. Therefore it is useful to characterize the circuit performance in terms of the energy dissipated in the switch. Equation 4 gives E_{switch}. Figure 5 is a plot of the dissipation fraction δ defined as the ratio of energy dissipated in the switch to the total inductively stored energy

$$\delta = \frac{L_o}{L_s + L_o} \tag{13}$$

Equation 13 indicates that δ is a function of ΔL through L_s when L_s is optimized by Equation 11, and is therefore a relatively weak function of ΔL. For small ΔL the curve approaches 50 percent, as expected for a static load. The significance of δ is that it represents the minimum amount of energy that will be dissipated when the switch opens, regardless of the characteristics or relative time of the operations of switch S_1 and switch S_2. Conversely, it is the minimum energy available to actuate a dissipation
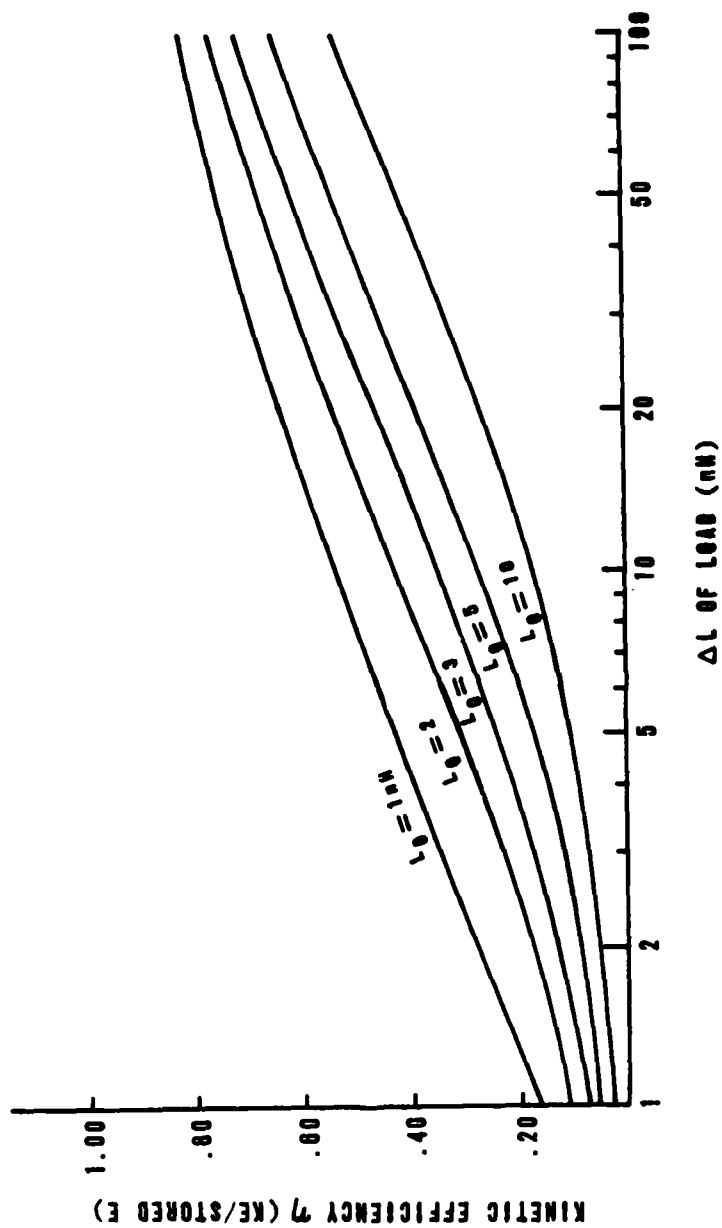
9

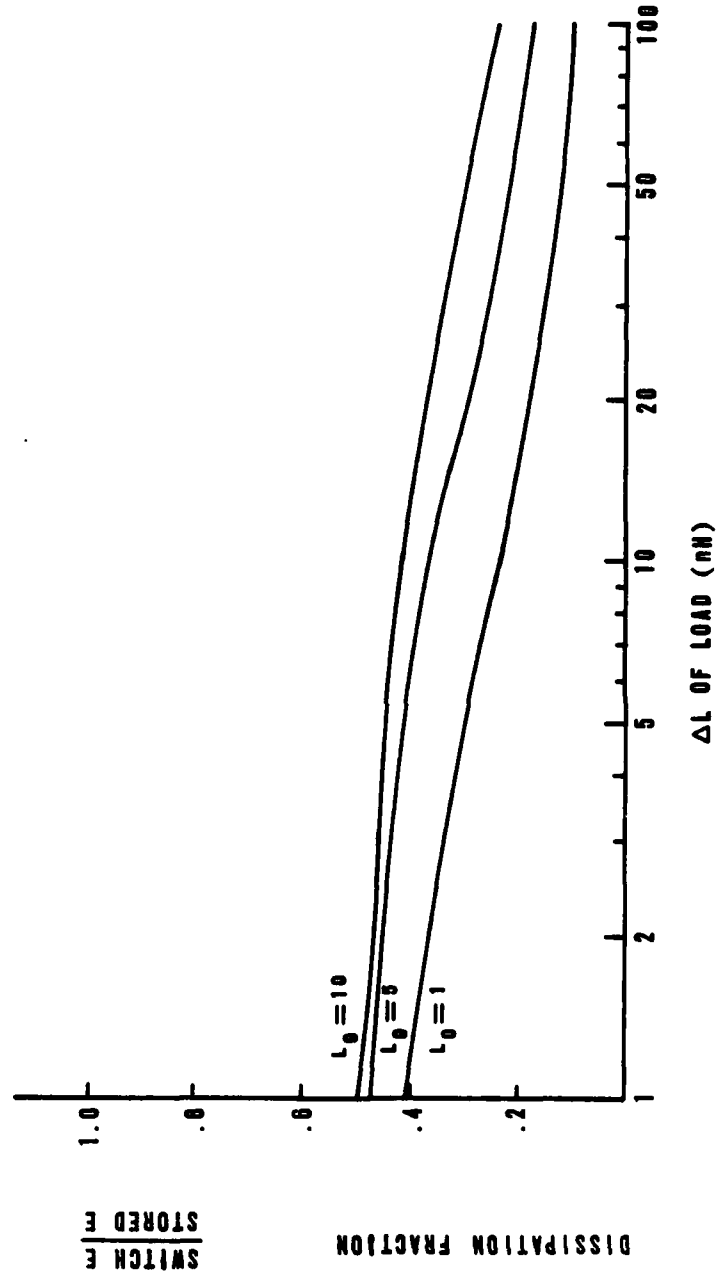Figure 4. Kinetic efficiency vs change in load inductance.

Figure 5. Dissipation factor vs change in load inductance.

driven switch. There is a temptation to develop a switch which requires very
little energy. Figure 5 indicates that, for example, for $L_0 = 3$ nH and
$\Delta L - 12$ nH, almost 40 percent of the energy must go into the switch, regard-
less of how clever the design.

Since dissipatively operated current interrupting switches are likely
candidates, and since a dissipative switch may require more than the minimum
energy δ, the fraction f of the inductively stored energy coupled to kinetic
energy after switching is also a relevant parameter. Using Equations 2, 3,
and 7

$$F = 1 - \frac{L_s + L_0}{L_s + L_0 + \Delta L} \tag{14}$$

Figure 6 is a plot of the coupling fraction f. The plot shows that, for
realistic values of 3 nH $< L_0 <$ 5 nH for ΔL of 12 nH, approximately half the
energy remaining after switching is coupled to kinetic energy.

When S_1 opens and S_2 closes, the current flowing in the charging circuit
falls from I_0 to the value given by Equation 2.

$$I_1 = \left(\frac{L_s}{L_s + L_0}\right) I_0$$

The current in the load rises from 0 to I_L. The rate at which the load
current rises may be important from the standpoint of MHD stability of the
imploding plasma. If the switch resistance rises from $R_s = 0$ to $R_s = R$
instantly (a step function), and if a form $I_L = I$, $(1-e^{-\alpha t})$ is assumed for
I_L, then we observe from Figure 2 that the voltage across the resistor
(a short time Δt following the step increase in resistance) is

$$V_R = I_0 R = L_L \frac{dI_L}{dt} \tag{15}$$

Thus

$$\frac{dI_L}{dt} = \frac{I_0 R}{L_L} = \alpha I_1 e^{-\alpha t} \tag{16}$$

For $e^{-\alpha t} \approx 1$,

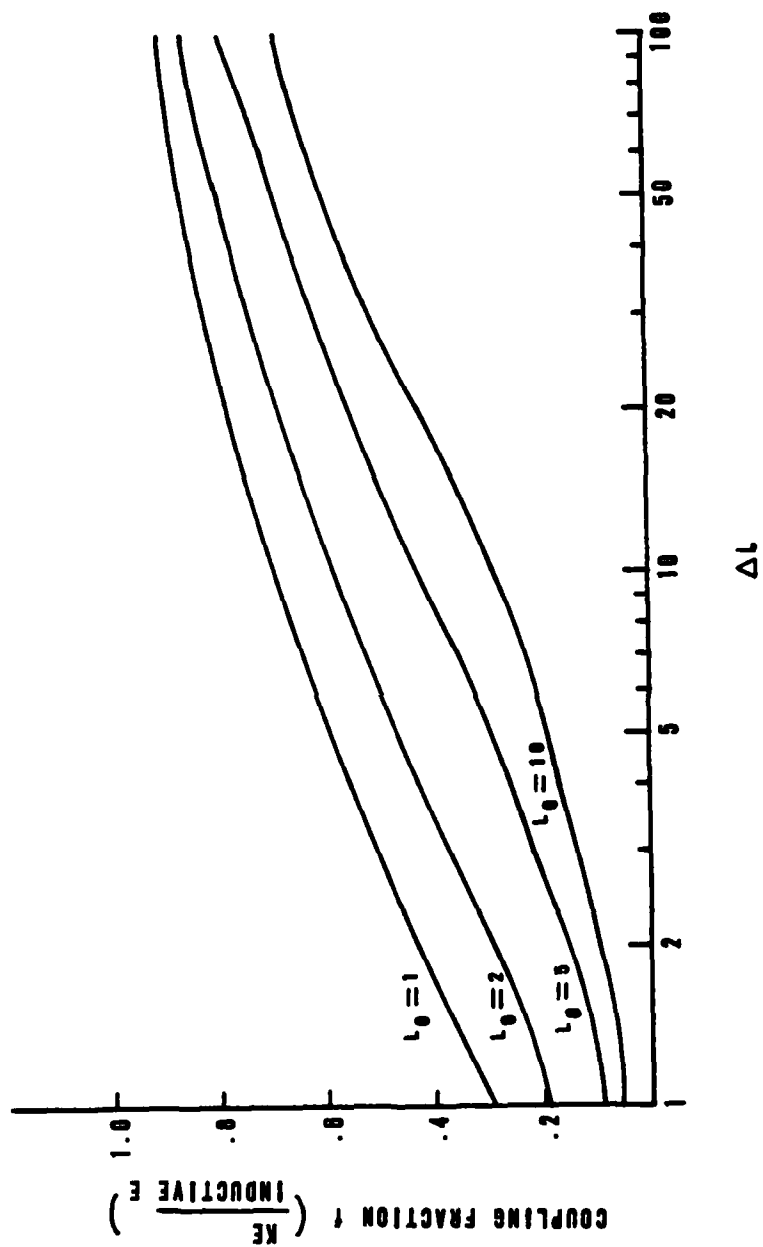$$\alpha = \frac{I_0}{I_1} \frac{R}{L_1} \tag{17}$$

12

Figure 6. Coupling fraction vs change in load inductance.

13

or by Equation 2,

$$\alpha = R\left(\frac{L_s + L_o}{L_s L_o}\right) \tag{18}$$

The time constant reflected in Equations 17 and 18 may also be found by simultaneously rating the two loop equations for the current in Figure 2. That solution verifies both the assumed form of I, and the value of α. For very large values of R, the rise time in the load is very short. For example, if $R = 1 \, \Omega$ and $L_o = 5$ nH, $L_s = 10$ nH, $\alpha = 0.3 \times 10^9$, the current rise time would be 3 ns.

From this simple analysis, design criteria emerge:

a. Minimize L_o.

b. Choose $L_s \approx \sqrt{L_o^2 + L_o \, \Delta L}$.

c. Maximize ΔL, but not by increasing h if kinetic per unit length is a concern.

d. A significant amount (at least 25 percent in most cases) of energy will be dissipated in the switch, placing a lower limit on the switches dissipation rating.

This analysis makes a number of assumptions:

a. Infinite final resistance of the opening switch is assumed. In a crude attempt to quantify "infinite," the final resistance of the switch must be large compared to the highest impedance presented by the load to prevent significant current sharing through the switch. The $\dot{L}$ component given by

$$\dot{L}_{(t)} = \frac{\mu_o}{2\pi} \, h \, \frac{v_{(t)}}{r_{(t)}} \tag{19}$$

(where v and r are velocity and position, respectively, of the foil) is the largest contributor to the load impedance. Thus, achieving a final switch resistance much greater than $\dot{L}$ is a possible criterion.

b. It was assumed that the resistance rises quickly. Quantitatively quickly implies that

$$\Delta t_{switch} \ll \Delta t_{implosion} \tag{20}$$

14

c. It is assumed that the output switch S_2 is closed when the resistance of S_1 begins to rise. Since total time of current flow in the load may be a determiner of foil/plasma stability, it may be desirable to close the switch later, thereby achieving higher initial voltages at closure time and hence presumably a higher initial $\dot{I}$ in the load.

III. CIRCUIT CALCULATIONS

The assumptions outlined in Section II place severe constraints on system components, especially on the opening switch. The validity of the requirements placed by the constant flux model can be evaluated using a more detailed circuit model. In this section, the numerical solution to a circuit similar to that in Figure 1 will be discussed. For numerical solutions, values were chosen for circuit elements which correspond to the parameters of the SHIVA-I capacitor bank systems as shown in Figure 7.
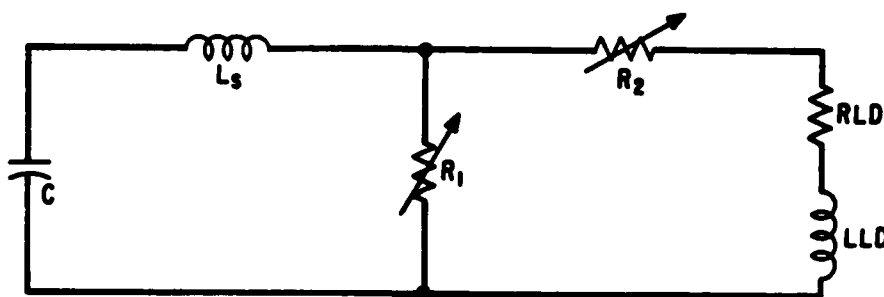
Figure 7. Circuit used for numerical circuit solutions.

The capacitor is 267 μF, charged to 120 kV storing 1.9 MJ. The load is modeled as a time changing inductance with values

$$LLD = \frac{\mu_o}{2\pi} \ h \ \ln \ \frac{R}{r_{(t)}} \tag{21}$$

where R is the radius of the return conductor and $r_{(t)}$ is the initial radius of the imploding foil; and the time varying resistance has a value of

$$RLD = \frac{\mu_o}{2\pi} \ h \ \frac{V_{(t)}}{r_{(t)}} \tag{22}$$

where $V_{(t)}$ is the velocity of the imploding cylinder. The coupled differential equations of motion

$$\ddot{r} = \frac{\mu_o}{4\pi m r_{(t)}} \ h \ I^2_{(t)} \tag{23a}$$

$$\dot{r} = V \tag{23b}$$

16

complete the set that is to be solved numerically. The initial foil radius was chosen at 5 cm and the height at 2 cm for stability reasons. The return conductor radius was chosen at 17.5 cm to give an initial value for the LLD of 5 nH, which correspond to L_0 = 5 nH in the analytic model. The assumption of 20:1 conversion leads to a minimum radius of 2.5 mm, a final value LLD of 17 nH, and a ΔL of 12 nH. Thus from L_0 and ΔL a value of the storage inductance is chosen from Equation 11 to be 9.2 nH. The series output switch is modeled as R_2, which is given as a time varying resistor whose value is 1 MΩ prior to switching time T_s and changes to 0.1 mΩ in 5 ns subsequent to T_s. The current interrupting switch is R_1, whose value is varied as a problem variable. The resistance of R_1 is arbitrary and is not computed from a material model for this analysis. The circuit was subjected to numerical analysis using a circuit solving code called Sceptre for a variety of R_1 profiles and time scales and for a variety of switch times T_s.

TERMINAL RESISTANCE

For the circuit in Figure 7 with L_0 = 5 nH, and ΔL = 12 nH, the efficiency from Figure 4 is 30 percent. Assuming all capacitively stored energy (1.9 MJ) is transferred to the inductance L_s, the coupled kinetic energy should be 570 kJ. With a desired final velocity of 33 cm/µs, the total foil mass should be approximately 1 x 10^{-5} kg, or 161 µg/cm^2. At 33 cm/µs final velocity and 2.5 mm final radius, the final $\dot{L}$ is 0.5 Ω. The implication of the constant flux model was that the final valued R_1 should be much greater than 0.5 Ω to assure that most of the current is flowing in the load. To model the situation, the resistance profile shown in Figure 8 was imposed on R_1.
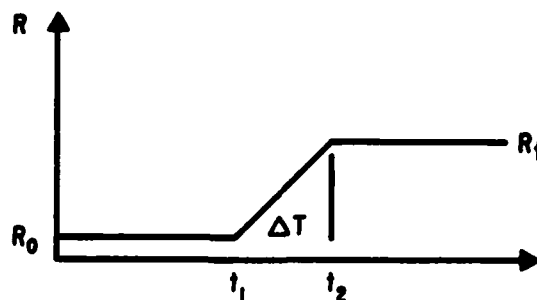

Figure 8. Time dependence of resistance at opening switch.

17

Where R_0 was taken as 0.0 and T_1 was taken as the time of peak current,

$$T_1 = \frac{\pi}{2} \sqrt{L_s C} = 2.46 \ \mu s \qquad (24)$$

To assure that $\Delta t \ll t_{imp}$, Δt was taken as 100 ns and R_f was varied from 30 mΩ to 5 Ω. The time at which the output switch closed T_s, was a constant at 2.465 μs. Figure 9 shows a plot of the kinetic energy coupled to the imploding foil and the final velocity of the foil when it had collapsed to a radius of 2.5 mm as a function of R_f, the final switch resistance. As anticipated, the kinetic energy coupled at lower values of R_f is lower than that observed at higher values. Somewhat surprising is the fact that when $R_f \approx \Omega/2$ (peak $\dot{L}$), nearly 90 percent of the kinetic energy predicted by the flux model was observed coupled in the numerical solution; but when R_f drops more than an order of magnitude to 30 mΩ the kinetic efficiency decreases only moderately to 62 percent of the efficiency predicted by the flux model. This relatively moderate impact of changing R_f can be motivated by referring to Figure 10 where RLD and $R_{1(t)}$ are plotted as functions of time for the case where $R_f = 30$ mΩ. The plot shows that the dissipative part of the load impedance RLD rises rapidly at the very end of the implosion, and even for a very modest value for R_f, RLD is less than R_f for about 90 percent the implosion time. Although most of the kinetic energy is coupled late in the implosion, note that once transferred to the inductance LLD, energy will tend to dissipate more rapidly in the larger resistance (RLD) because of the shorter L/R times. In other words, the energy lost in R_1 is $I^2 R_1 \Delta t$ (where Δt is very short), and thus can account for only a small fraction of the inductively stored energy. Thus, since RLD is much less than R_f for most of the implosion, efficient coupling to LLD is achieved, and most of that energy is still made available to the implosion. Conceptually carrying this logic to the extreme, the switch operation could be carried out, energy stored in L_0, and R_1 could even be crowbarred while the foil implodes. A lower limit on kinetic efficiency η_{ke} can be found by considering Equation 3 for the total energy after switching $E_1 = (L_s/L_s + L_0) E_0$. The fraction stored in L_0 is

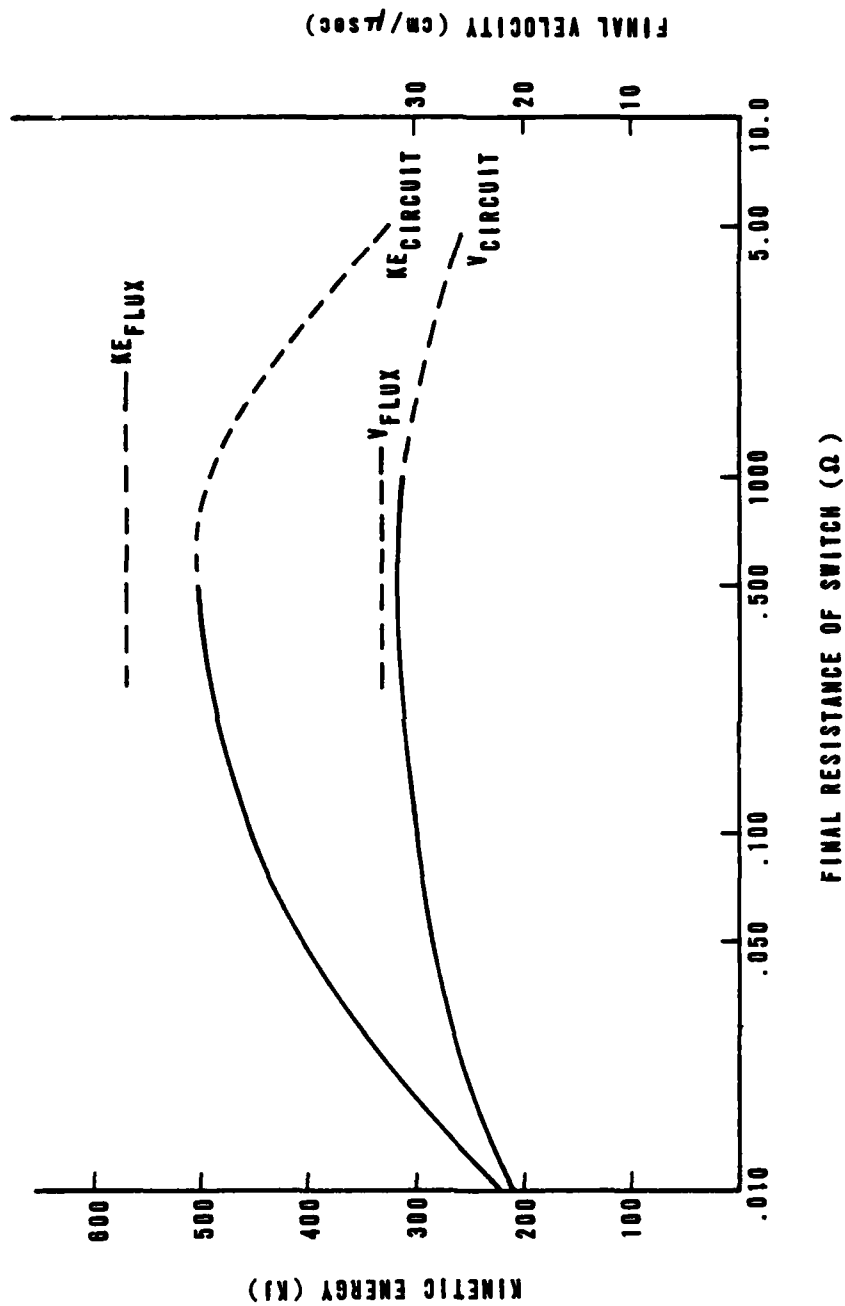$$E_{L_0} = \frac{L_s L_0}{(L_s + L_0)^2} E_0 \qquad (25)$$

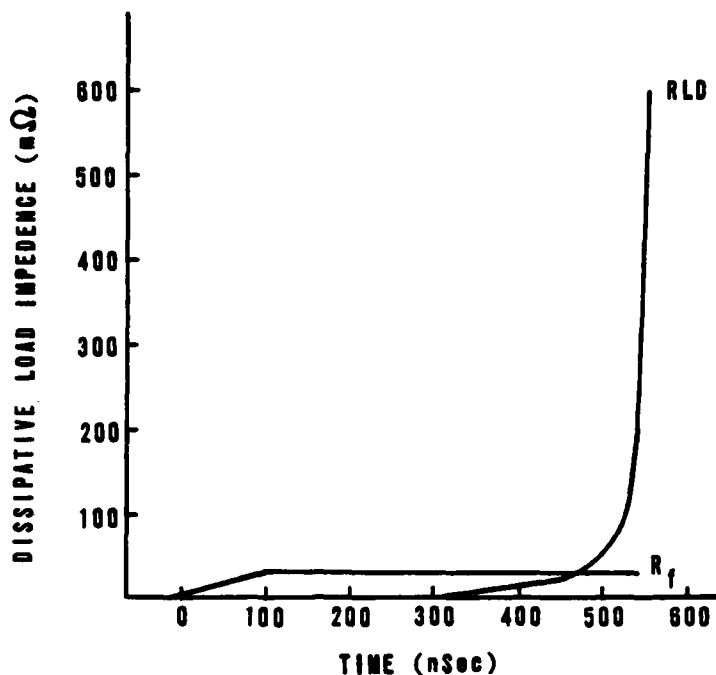Figure 9. Kinetic energy and velocity vs switch resistance.

19

Figure 10.   Load L vs time.

And the energy coupled to kinetic energy is

$$\left(1 - \frac{L_0}{L_0 + \Delta L}\right) E_{L_0} = \frac{\Delta L}{(L_0 + \Delta L)} \frac{L_s L_0}{(L_s + L_0)^2} E_0 \tag{26}$$

$$\eta_{CB} = \frac{L_s L_0 \Delta L}{(L_0 + \Delta L)(L_s + L_0)^2} \tag{27}$$

For $L_0 = 5$ nH, $\Delta L = 12$ nH, and $L_s = 9.2$ nH,

$$\eta_{CB} = 16 \text{ percent} \tag{28}$$

For $R_f = 10$ mΩ, Figure 9 shows η_{ke} is even less than the crowbarred efficiency. This is explained by realizing that in the case of very low R_1, current transfer to the load is never complete. The implication is that if high final fuse resistance is not easily achievable, a crowbarred case when R_f goes temporarily high and then collapses may be preferable to a lower fuse resistance.

20

Figure 9 also exhibits a falloff of η_{ke} above approximately 0.5 Ω. This result, perhaps more surprising than the relatively moderate falloff at low R_f, is explained by referring to Figure 11 where the energy dissipation in the fuse at T = 2.56 μs, the time when the resistance stops rising, and the energy dissipated in the fuse at pinch time are plotted as a function of R_f. The simple analysis indicates that 670 kJ is the minimum energy that must be dissipated in the fuse. For values of R_f between 100 mΩ and 1 Ω, the circuit puts most of the dissipated energy into the fuse during the opening time, and little energy into it during the implosion. This behavior is similar to that of the simple analysis. This range also corresponds to the region of peak kinetic energy shown in Figure 9.

At larger values of R_f, Figure 11 shows that excessive energy is dissipated in the fuse during opening time, thus leaving less energy in the magnetic circuit to drive the implosion; this explains the lower overall efficiency. The excessive energy deposited at high values of R_f was investigated. Decreasing the closing time of the series output switch R_2 resulted in improved efficiency and decreased dissipation at large values of R_f. In fact, the kinetic energy approaches the 670 kJ flux model value. Presumably when $\dot{R}$ is very large (i.e., R_f is large and Δt is fixed), excessive energy is dissipated in R_1 prior to the closing of R_2. Actually the 5 ns value of R_2 used to generate the data in Figure 9 is more representative of practical multichannel switches than the < 1 ns value required to achieve flux model efficiency. The implication is that low jitter output switching is required if very large values of R_f are used. Moderate values of R_f do not place severe limitations on R_2 performance. The conclusion is that, for implosion parameters discussed, values of R_f that are greater than the initial $\dot{L}$ of the load (a few milliohms), but not much greater than the final $\dot{L}$ (one-half ohm) performance, seem to be predicted by the simple model within about 20 percent. Thus the criteria result

$$\dot{L}_o >> R_f \sim \dot{L}_{pinch} \tag{29}$$

OPENING TIME

The simple flux model presumes that the implosion is carried out in two steps. First a current interruption occurs; then an implosion phase occurs. The energy transfer is calculated on the assumption that $L_{(t)}$ does not change
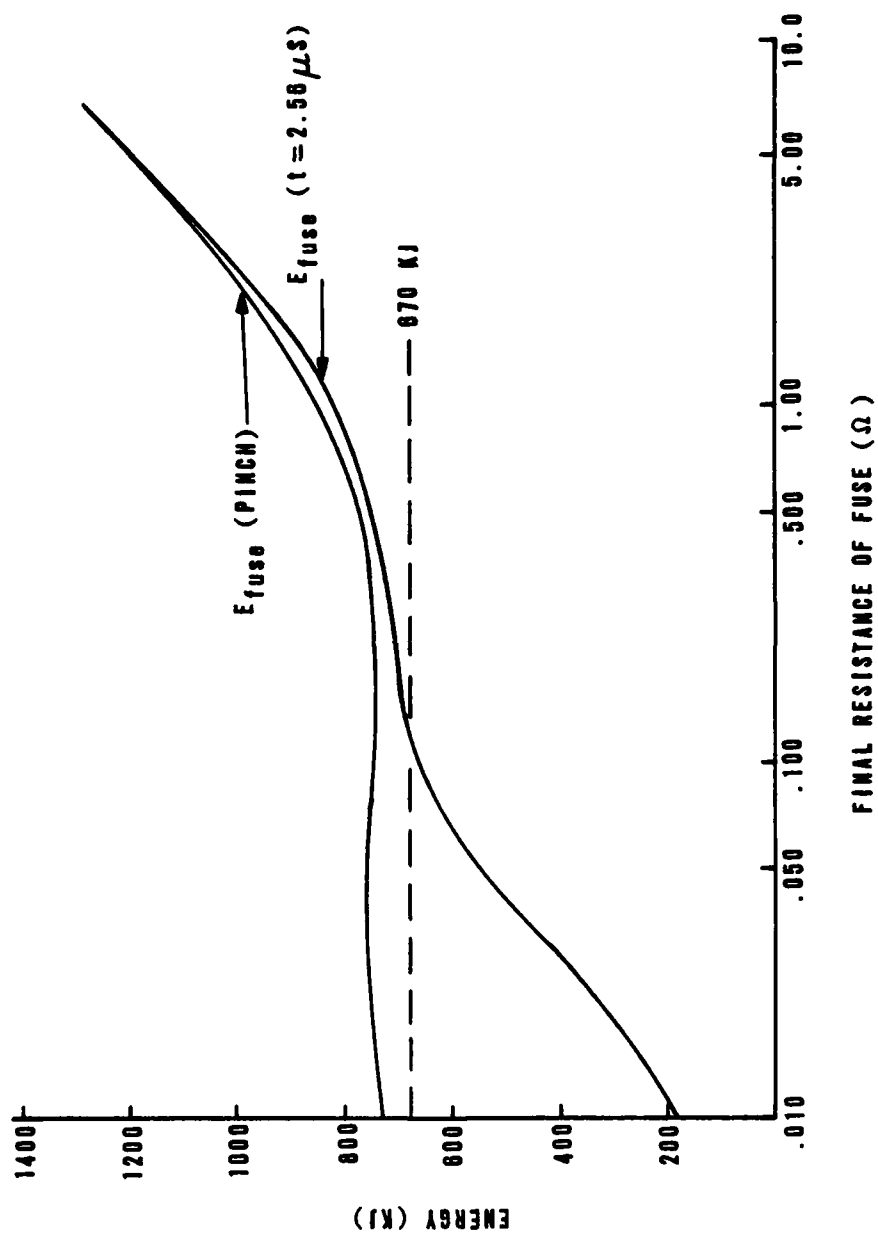
Figure 11. Dissipated energy vs time.

during the interruption phase; that is, the calculation assumes switching into a static load. Figure 12 is a plot of LLD vs time for a case where R_f = 100 mΩ, ΔL = 12 nH, L_0 = 5nH, L_s = 9.2 nH, and ΔL = 100 ns. During the 300 ns following output with closure at 2.465 μs (2.465 to 2.765 μs), the inductance of the load LLD rises about 25 percent. Thus, for time scales of about three-fourths of the implosion time, the opening switch is seeing a nearly constant $L_{(t)}$ approximately equal to $L_{(t = 0)}$. Figure 13 is a plot of kinetic energy coupled for a 20 to 1 compression vs the ramp time of the switch impedance. The final value R_f is 100 mΩ. The plot shows virtually no change of efficiency for time scales up to 300 ns, which is very close to 75 percent of the implosion time. For time scales up to 500 ns, the loss of efficiency is less than 5 percent and the implosion time lengthens somewhat (from 450-550 ns). For ramp times (Δt) longer than 500 ns, the switch can be thought of simply as a 500-ns ramp of lower $\dot{R}$ and thus a lower R_f. The effect of lowering R_f is shown in Figure 9.

IMPLOSION MASS/FINAL VELOCITY

One of the advantages of inductively driven implosion systems is that, at least in the simplest model, the kinetic energy coupled is dictated only by the inductance ratios and is independent of the implosion mass. This allows relatively wide variations in final velocity to be achieved independently of kinetic energy, and hence allows assessment of the effect of final velocity on the thermalization process. Figure 14 is a plot of the kinetic efficiency, final velocity, and implosion time as a function of implosion mass. The plot shows that, for a full order of magnitude change of implosion mass (5×10^{-5} to 5×10^{-6} kg), the change in kinetic energy is small while the change in velocity is given by the anticipated $\sqrt{10}$ from 11.9 cm/μs. As expected, the implosion time varies over a similarly wide range associated with the changing final velocity. For very large masses and for very small masses, the kinetic efficiency suffers somewhat. The numerical solutions show that for the large masses the long implosion time leads to reverse charging of the bank capacitance (because a relatively large current is flowing in the positive direction for a long time after current peak). The energy stored in the recharging capacitor is approximately three times the observed loss in kinetic energy. For small values of mass (hence short implosion time), loss results from effective lowering of the fuse resistance caused by early pinch.
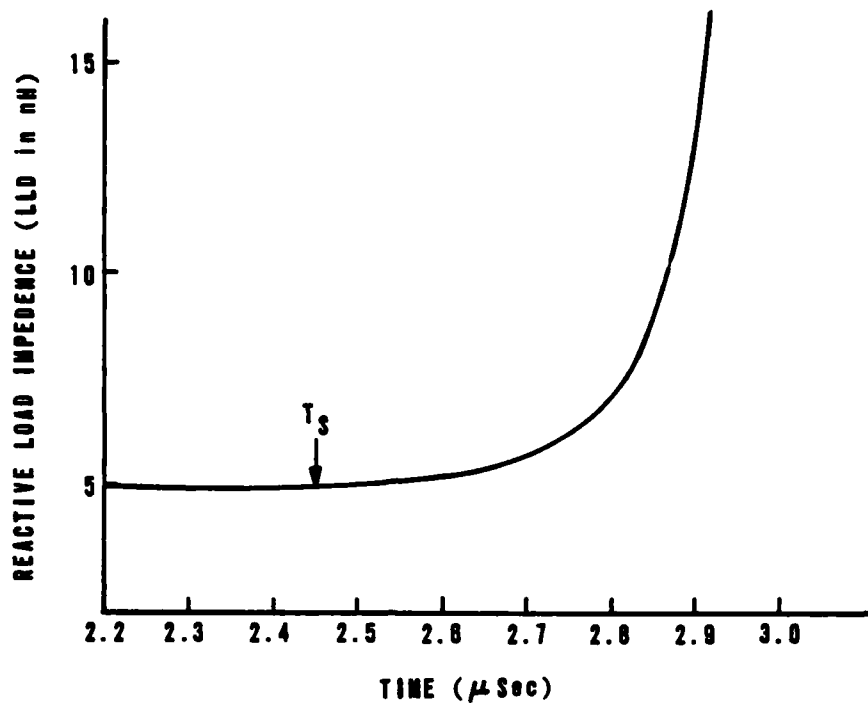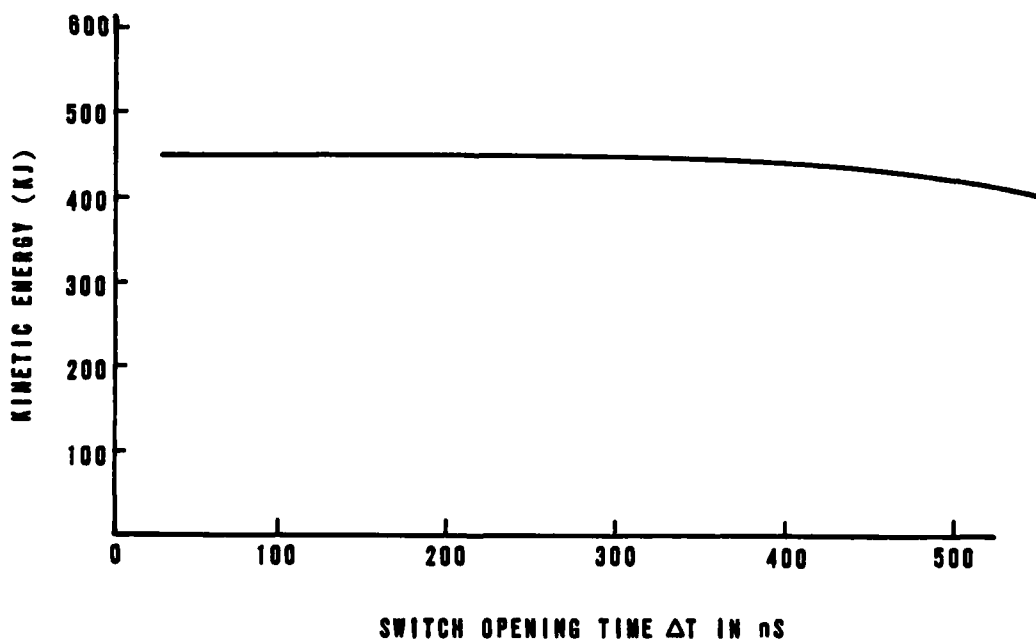
23

Figure 12.   Load L vs time.
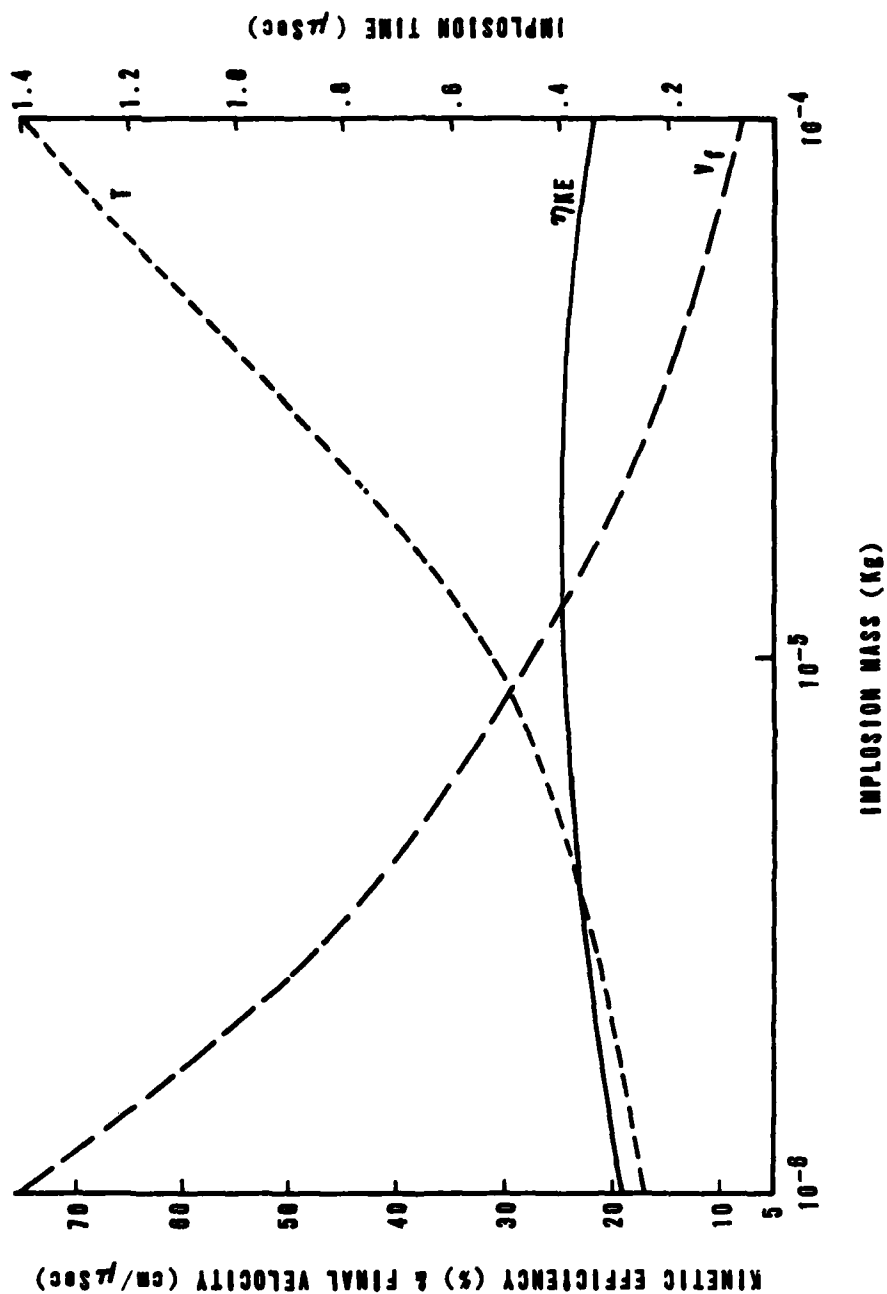

Figure 13.   Kinetic energy vs rise time.

24

Figure 14. Implosion parameters vs mass.

OUTPUT SWITCH CLOSURE TIME

The time at which the output switch closes is expected to impact the total kinetic efficiency. For example, closing the output switch late in the interruption may be expected to result in excessive energy deposition in the fuse and hence lower kinetic efficiency. On the other hand, closure of the output switch too early may be expected to result in lower voltages across the load (and hence lower initial $\dot{I}$) and perhaps a longer implosion time for a given load.

Figure 15 shows a plot of η_{ke} and implosion time as function switch time T_s for a case where R_f equals 500 mΩ. The implosion mass was 1×10^{-5} kg, and the switch opening time Δt was 100 ns. For reference, the fuse resistance profile is also sketched. The figure shows that both kinetic energy and implosion time are sensitive to switch closure time. As expected, kinetic energy drops and implosion time increases with later closing time. Implosion time shows a tendency to flatten out for closure time near the start of the interruption (2.46 μs). Fortunately, from a practical point of view, the earliest possible closure time (after start of interruption time) appears most promising from both the point of view of efficiency and of implosion time. This suggests that a self-breaking switch set to close at low (perhaps a few $\times 10^4$ V) may be adequate. The difficulty is that of achieving low inductance multichannel performance with low-voltage self-breaking switching.

INITIAL FUSE RESISTANCE

Two cases were compared with R_f = 100 mΩ; one with R_i = 0 and one with R_i = 1 mΩ. Significantly less (300 kJ) kinetic energy was observed with R_i $\sim$ 1 mΩ then with R_i = 0. On the other hand, peak storage current was also reduced, as expected with the larger values of R_i; but the kinetic efficiency was virtually identical in the two cases. The conclusion is that kinetic efficiency is virtually independent of changes in the ratio R_f/R_i.

RESISTANCE SHAPE

The linear ramp is conceptually the easiest to examine, but is not necessarily the most accurate representation of resistivity data. A number of profiles were compared, each of which rose from R_i = 0.1 mΩ to 500 mΩ
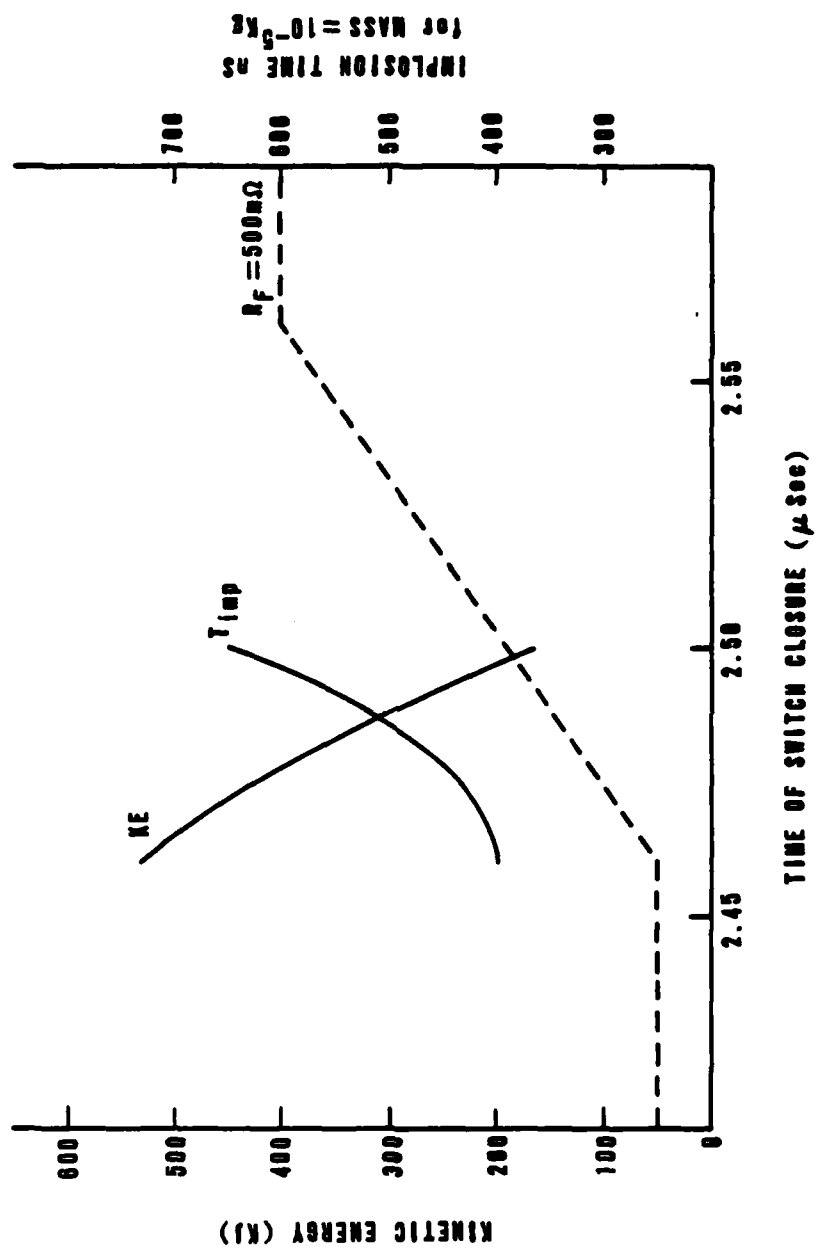
Figure 15. Implosion parameters vs switch time.

in Δt = 200 ns. The ramp profile was compared with a smoother S-shaped curve, a square low profile, and an exponential. All four profiles produced from 488-523 kJ coupled kinetic energy or a 7 percent variation. The linear ramp produced less kinetic energy than either the S shape or the exponential, and slightly more than the square low profile.

IV. SWITCH TECHNOLOGY

Finally, it is appropriate to consider the prospects for the success of a high-energy inductive store/opening switch system as a driver for a practical imploding plasma load. Significant data have been published on the behavior of exploded foil fuses used as opening switches; but in general the energy level (25 kJ) and the time scale (10 to a few hundred μs) are not representative of the behavior of the fusing element in systems of interest (2 MJ, 1-2 μs). The work most nearly approaching these parameters is that already performed by the Air Force Weapons Laboratory (AFWL) at the 100-kJ, 3-4-s level (Ref. 2). This section examines the results of this work in light of the foregoing analysis and circuit calculations.

Figures 16 and 17, extracted from Reference 2, show current and voltage profiles for a set of copper foil fuses quenched in glass beads for a variety of physical lengths and widths which maintain a constant total fuse mass of 25 g (for 1 mil thickness). Based on preceding analysis, the most promising choice for a fuse might be one which produces the highest storage current while still opening in times less than (but not necessarily much less than) the implosion time. From the data, it is clear that (for this family) opening time must be compromised against peak current. It is also clear that opening time does not have a simple interpretation. It is convenient to accept the FWHM of the voltage pulse to measure quality of the switch. Consideration of the simple L-R circuit shows that the FWHM of the voltage pulse is composed of two parts. The rise time is related to the rise time of the fuse resistance. In the simplest case of a step function resistance, the voltage rise is also a step; however, the fall time is related to the L/R decay of the circuit L and the final switch resistance R. Thus, a sharp rising pulse with a fast decay indicates both rapid dR/dt and high final resistance, hence a better quality switch.

2. McClenahan, et al., 200 Kilojoule Copper Foil Fuses, AFWL-TR-78-130, Air Force Weapons Laboratory, Kirtland Air Force Base, New Mex, (to be published).
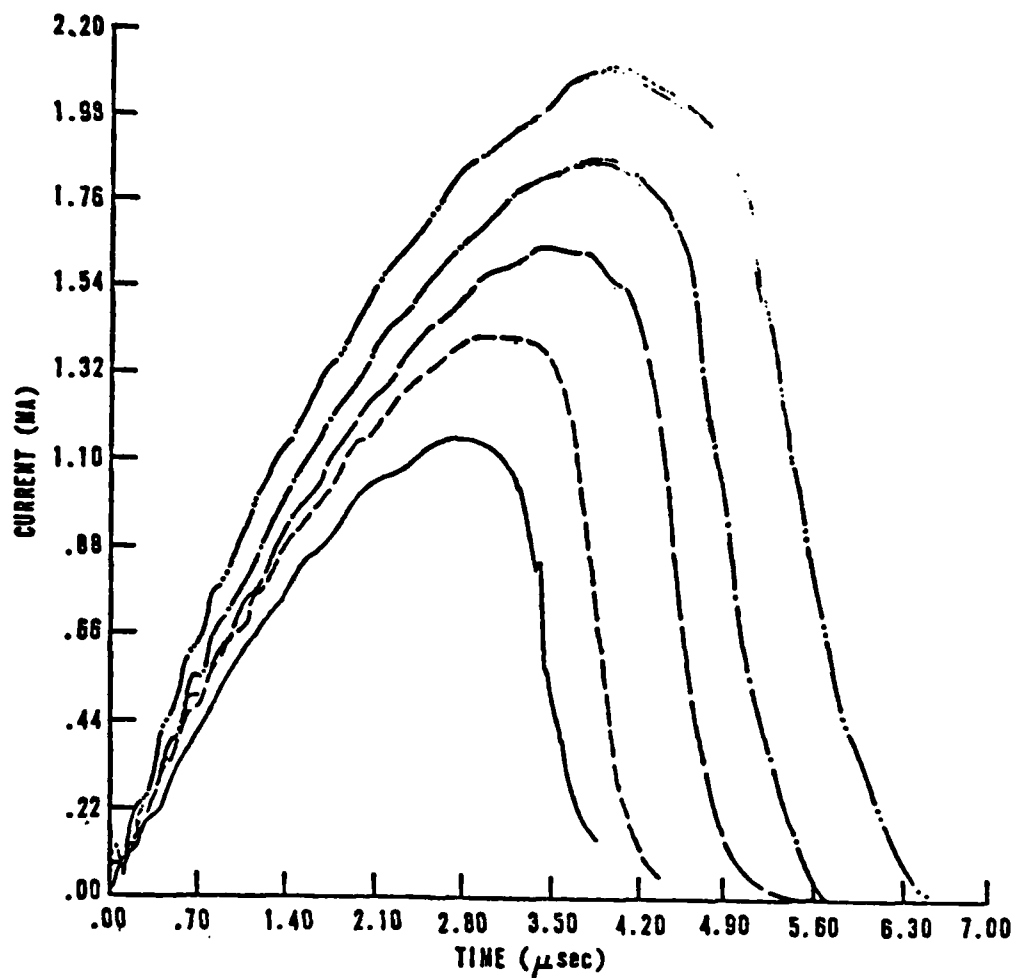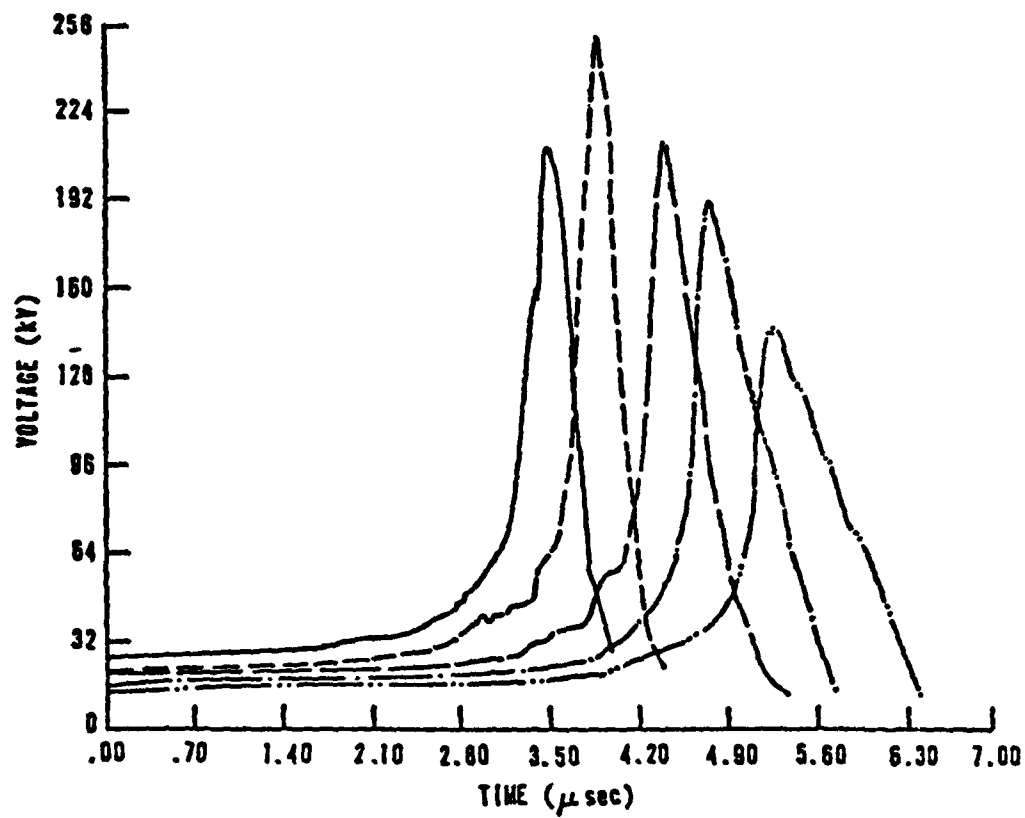
Figure 16. Fuse current data.

Figure 17. Fuse voltage data.

Figure 15 shows that the shortest interrupt time is associated with the peak voltage (maximum I) but not with the maximum storage current; thus, compromise is in order. For this analysis, the maximum voltage case is discussed. The FWHM of this case is 370 ns, which is acceptable for driving a 400-450 ns implosion.

For scaling purposes, resort to Massionier's and DeMarcu's analysis (Refs. 3 and 4), suggest a cross-sectional area for a fuse based on the parameters of the driving circuit and on the physical properties of the fuse material of interest.

$$s^2 = \frac{W^{3/2}}{V \, L^{\frac{1}{2}} \, k_1 a} \tag{30}$$

where

s = cross section of fuse (m^2)

W = stored energy (J)

L = total system inductance (H)

V = charge voltage of capacitor bank (V)

$k_1 a$ = set of parameters describing the material; $k_1 a = 1.2 \times 10^{17}$ (copper)

For the data in Figures 16 and 17,

W = 200 kJ

V = 50 kV

L = 67 nH

Thus, Equation 30 would predict

$s = 7.6 \times 10^{-6} m^2$

$= 0.076$ cm^2 $\tag{31}$

The fuse in question was 21 cm wide and 0.001" thick or

$s^2 = 0.053$ cm^2

or roughly 70 percent of that predicted by Massionier model.

---

3. Massionier, et al., "Rapid Transfer of Magnetic Energy by Means of Exploding Foil," Rev. Sci. Instr. 37, No. 10, 1966.

4. DeMarcu, Berkhart, "Characteristics of a Magnetic Energy Storage Switches Using Exploding Foils," Rev. Sci. Instr. 41, No. 9, 1970.

Scaling upward for a system where

W = 2 MJ
V = 120 kV
L = 9.2 nH

The predicted area is 0.45 cm or s^2 = 0.32 cm. For interest, a foil 1 mil thick would then be only 1.3 m wide.

Figure 18 shows a plot of material resistivity, ρ, versus specific energy dissipated in the fuse. The functional relationship between ρ and specific energy is open to question, but for simple approximations we will take the empirical data of Figure 18. Recalling that the previous analysis (Fig. 11) indicated that a maximum of 670 kJ must be dissipated in the fuse, and taking approximately 6 kJ/g as the upper limit of useful specific energy from Figure 18, indicates that 112 g of material could be utilized. At a density of 8.9 g/cc and a cross section of 0.32 cm^2, this implies a fuse length of 40 cm. If the fuse reaches a maximum resistivity of 520 $\mu\Omega$ cm, the fuse that is 0.32 cm^2 x 39 cm has a peak resistance of 63 mΩ. From Figure 9, a fuse with R_f of 63 mΩ would drive an implosion to better than 400 kJ of kinetic energy or 20 percent overall kinetic efficiency. The initial resistivity of this fuse would be 0.2 mΩ, which is much less than the 1 mΩ value found to be a realistic maximum initial R_i. Note that the interpretation attached to the data in Figure 18 is pessimistic because the resistivity curve appears to be clearly steepening (not yet having reached the plateau assumed in the model of R_f). On the other hand, Figure 9 shows that, while increasing resistivity (or increasing R_f) will help somewhat, the marginal gains are small.
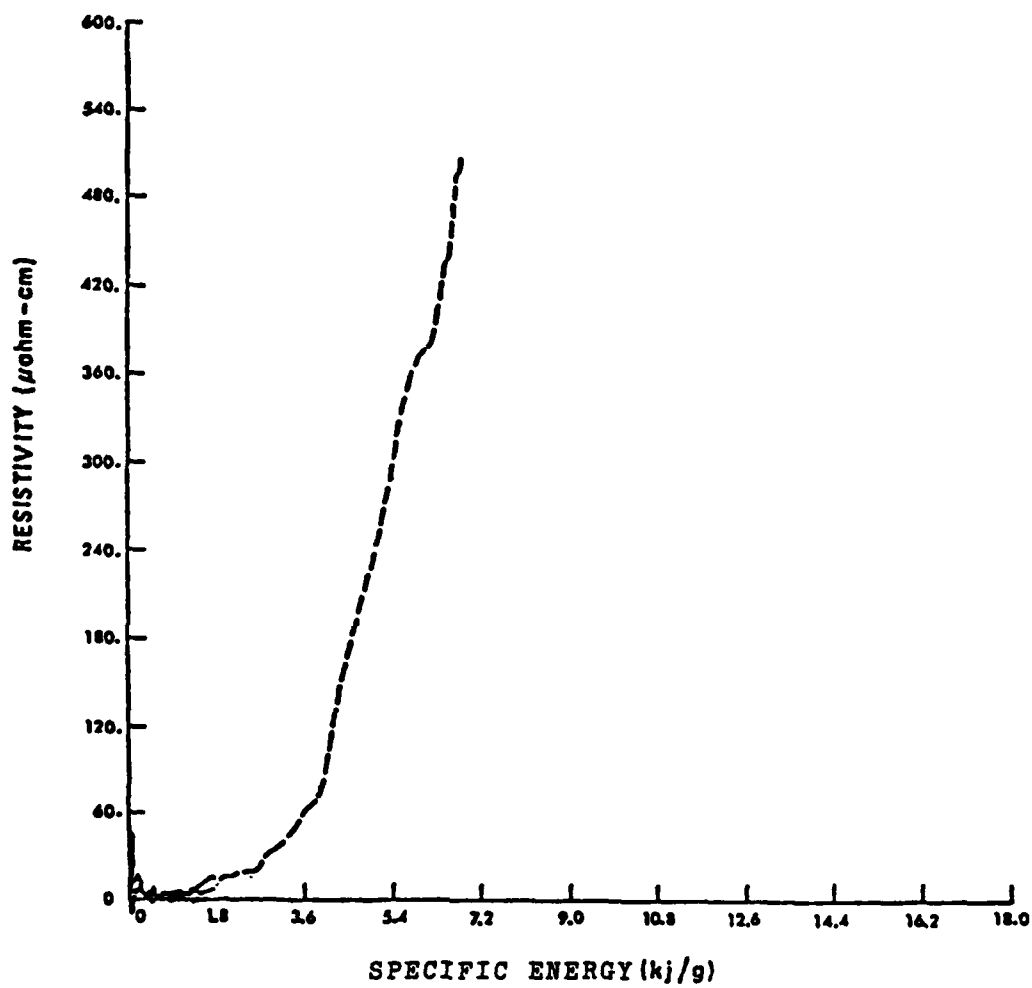
Figure 18.   Fuse resistivity data.

V. CONCLUSIONS AND RECOMMENDATIONS

In conclusion, simple extrapolation of already existing data leads to a conceptual design for a fused opening switch which can be implemented on a 2-MJ system. The resulting plasma implosion should be compared against that which can be obtained by directly driving the plasma from the capacitive energy storage. Using an initial geometry of 7-cm radius and 2-cm height, and requiring for stability reasons that the direct driven implosion be complete in less than 1.4 μs, results in the coupling of approximately 400 kJ of kinetic energy to the implosion be the direct case. This compares very favorably with the 400 kJ of kinetic energy implied in the above analysis. The advantage of the inductive system is clearly the time scale on which the energy is delivered. The inductive system promises 400-ns implosions, a factor of more than 3 faster than the 1.4 μs direct-driven implosions. Apparently significant gains can be achieved by this fairly modest reduction in implosion time.